

Metrics for linking emissions of gases and aerosols to global precipitation changes

K. P. Shine et al.

This discussion paper is/has been under review for the journal Earth System Dynamics (ESD). Please refer to the corresponding final paper in ESD if available.

Metrics for linking emissions of gases and aerosols to global precipitation changes

K. P. Shine¹, R. P. Allan¹, W. J. Collins¹, and J. S. Fuglestad²

¹Department of Meteorology, University of Reading, Reading, UK

²CICERO – Center for International Climate and Environmental Research – Oslo, Oslo, Norway

Received: 13 March 2015 – Accepted: 18 March 2015 – Published: 2 April 2015

Correspondence to: K. P. Shine (k.p.shine@reading.ac.uk)

Published by Copernicus Publications on behalf of the European Geosciences Union.

Title Page

Abstract

Introduction

Conclusions

References

Tables

Figures

◀

▶

◀

▶

Back

Close

Full Screen / Esc

Printer-friendly Version

Interactive Discussion

Abstract

Recent advances in understanding have made it possible to relate global precipitation changes more directly to emissions of particular gases and aerosols that influence climate. Using these advances, a new index is developed here called the Global Precipitation-change Potential (GPP), which measures the precipitation change per unit mass of emissions. It is recognised that precipitation changes are predicted to be highly variable in size and sign between different regions, and ultimately climate change impacts will be more dependent on these regional changes. Nevertheless, the GPP presents a useful measure of the global-mean role of emissions of individual forcing agents.

Results are presented for pulse (GPP_P) and sustained (GPP_S) emissions for selected long- and short-lived forcing agents (CO_2 , CH_4 , N_2O , sulphate and black carbon – BC) using illustrative values of required parameters. The GPP can be used as a metric to compare the importance of emissions. This is akin to the global warming potential (GWP) and the global temperature-change potential (GTP) which are used to place emissions on a common scale. The GPP is further down the cause-effect chain from emissions to impacts than the GWP and GTP, and so provides an additional perspective.

One key parameter needed for the GPP is the surface–atmosphere partitioning of radiative forcing. Few studies have presented results for this partitioning for different forcings, leading to more uncertainty in quantification of the GPP than the GWP or GTP. Using CO_2 as reference gas, the pulse and sustained GPP values for the non- CO_2 species are larger than the corresponding GTP values, because the CO_2 GPP is the sum of two quite strongly opposing terms. For BC emissions, the atmospheric forcing is sufficiently strong that the GPP_S is opposite in sign to the GTP_S . The choice of CO_2 as a reference gas is problematic, especially for the GPP_S at time horizons less than about 60 years, because the opposing terms make the CO_2 GPP_S particularly sensitive to uncertainties in input parameters.

Metrics for linking emissions of gases and aerosols to global precipitation changes

K. P. Shine et al.

Title Page

Abstract

Introduction

Conclusions

References

Tables

Figures

◀

▶

◀

▶

Back

Close

Full Screen / Esc

Printer-friendly Version

Interactive Discussion



Metrics for linking emissions of gases and aerosols to global precipitation changes

K. P. Shine et al.

Title Page

Abstract

Introduction

Conclusions

References

Tables

Figures

◀

▶

◀

▶

Back

Close

Full Screen / Esc

Printer-friendly Version

Interactive Discussion



The GPP can also be used to evaluate the contribution of different emissions to precipitation change during or after a period of emissions. As an illustration, the precipitation changes resulting from emissions in 2008 (using the GPP_p) and emissions sustained at 2008 levels (using the GPP_s) are presented. These indicate that for periods of 20 years (after the 2008 emissions) and 50 years (for sustained emissions at 2008 levels) methane is the dominant driver of positive precipitation changes due to those emissions. For sustained emissions, the sum of the effect of the 5 species included here does not become positive until after 50 years, by which time the global surface temperature increase exceeds 1 K.

1 Introduction

A broad range of emissions of gases and aerosols influence climate, either directly or indirectly. That influence depends on the characteristics of the gases and aerosols, such as their lifetime, and their ability to influence the radiation budget. The conventional cause-and-effect chain links emissions to changes in concentrations, which then cause a radiative forcing with subsequent downstream effects on, for example, temperature, precipitation and sea level. By exploiting understanding of the characteristics of the gases and aerosol, in concert with simplified descriptions of the climate system, it is possible to develop simple methodologies that relate emissions directly to climate impacts, rather than having to explicitly account for the intermediate steps. Such methodologies have pedagogic value in making clearer the link between emissions (rather than, for example, concentration changes) and climate response and they also have potential applications. The purpose of this paper is to present a methodology that links global-mean precipitation directly to the emissions of different gases and aerosols. This exploits recent advances in understanding of how radiative forcing (RF) and temperature change influences precipitation change.

The impact of climate change depends on more than just global temperature change. Hence the development of a methodology linking emissions directly to precipitation is

Metrics for linking emissions of gases and aerosols to global precipitation changes

K. P. Shine et al.

Title Page

Abstract

Introduction

Conclusions

References

Tables

Figures

◀

▶

◀

▶

Back

Close

Full Screen / Esc

Printer-friendly Version

Interactive Discussion



attractive. However, precipitation change is much less amenable to a global representation than temperature change. Average surface temperature response to increased concentrations of greenhouse gases is largely the same sign over the whole planet, the temperature changes are coherent on large spatial scales, and climate models largely agree on the pattern of temperature change, if not the absolute size (e.g. Knutti and Sendlāček, 2012). By contrast, precipitation changes vary regionally in sign, are spatially much more variable and there is much less agreement between climate models on the patterns of response (e.g. Knutti and Sendlāček, 2012).

Part of the spatial variability in precipitation response is due to changes in atmospheric circulation in response to forcing, and also due to model internal variability. Nevertheless, for increased temperatures, there is a component of the precipitation response which has a regionally coherent pattern. Increases and decreases in precipitation are largely reflective of an amplification of precipitation minus evaporation fields, primarily explained by increasing concentrations of water vapour with warming (as expected from the Clausius–Clapeyron equation); this leads to systematic increases and decreases in precipitation depending on the region (e.g. Held and Soden, 2006; Liu and Allan, 2013). These changes are superimposed on a global-average increase in precipitation. Hence, when coupled with changes in temperature, changes in global-mean precipitation can be taken as being a useful an indicator of the size of disturbance of the global hydrological cycle.

The methodology presented here yields what we call the Global Precipitation-change Potential (GPP), which is the global-mean precipitation change per unit mass of emission. The GPP is presented for both pulse and sustained emissions. Section 2 presents the simple conceptual model that is used to relate precipitation change to RF and temperature change, which are themselves related to emissions. Section 3 presents some illustrative examples of the GPP drawing values of key parameters from the literature. Section 4 then uses the methodology in the context of climate metrics, and compares it with more conventional metrics – the Global Warming Potential (GWP) and Global Temperature-change Potential (GTP). Section 5 presents an illustration of the use of

Metrics for linking emissions of gases and aerosols to global precipitation changes

K. P. Shine et al.

Title Page

Abstract

Introduction

Conclusions

References

Tables

Figures

◀

▶

◀

▶

Back

Close

Full Screen / Esc

Printer-friendly Version

Interactive Discussion



the methodology for understanding the effects of emissions in an individual year (or sustained emissions from that year) on precipitation changes in or after that year – this illustrates the principle drivers of the precipitation change, given present-day emissions. Section 6 explores some aspects of the uncertainty in characterising the GPP and Sect. 7 discusses prospects for further developing the GPP.

2 Simple conceptual model

The simple conceptual model presented here originates from the analysis of simulated precipitation changes in response to increases in CO₂ presented by Mitchell et al. (1987). This analysis was based around the fundamental controls on the energy balance of the troposphere, in which, to first order, the latent heating resulting from the net rate of condensation of water vapour (and hence precipitation) is balanced by net radiative cooling. The conceptual model has been further developed more recently, and extended to both multi-model assessments and other climate forcing (and feedback) mechanisms (e.g. Allen and Ingram, 2002; Takahashi, 2009; Andrews et al., 2010; Kvalevåg et al., 2013; Allan et al., 2014).

The framework starts with an expression of the global-mean atmospheric energy budget, whereby the net emission of radiation by the atmosphere (i.e. the atmospheric radiative divergence (R_d), which is the sum of the emission of longwave radiation by the atmosphere minus the atmospheric absorption of longwave and shortwave radiation) is balanced by the input of surface sensible (SH) and latent (LH) heat fluxes so that

$$R_d = LH + SH. \quad (1)$$

LH is directly related to the precipitation as, at the global-mean level, evaporation (and hence LH fluxes) and precipitation approximately balance.

In response to the imposition of an RF and subsequent changes in temperature, humidity and clouds, R_d will change. The latent heat change ΔLH can then be written

$$\Delta LH = \Delta R_d - \Delta SH. \quad (2)$$

Metrics for linking emissions of gases and aerosols to global precipitation changes

K. P. Shine et al.

Title Page

Abstract

Introduction

Conclusions

References

Tables

Figures

◀

▶

◀

▶

Back

Close

Full Screen / Esc

Printer-friendly Version

Interactive Discussion



ΔL_H in $W m^{-2}$ can be converted to precipitation units of $mm day^{-1}$ by multiplication by 0.034 (86 400 s in a day divided by the latent heat of vaporisation, L ($2.5 \times 10^6 J kg^{-1}$ at 273.15 K)). There is some level of approximation in this conversion, as L is temperature dependent and some precipitation falls as snow rather than rain, and hence the latent heat of sublimation would be more appropriate. The precipitation change could also be quoted in % of total global-mean precipitation (about $2.68 mm day^{-1}$; e.g. Huffman et al., 2009).

ΔR_d has two components. The first component is due directly to the RF mechanism which can change the absorption of shortwave radiation and/or the emission and absorption of longwave radiation. The conventional top-of-atmosphere radiative forcing (RF) can be written as the sum of a surface component (RF_s) and an atmospheric component (RF_a), and it is RF_a that directly influences ΔR_d . It is convenient to relate RF_a to RF and so, following Allan et al. (2014), we define a parameter f such that $RF_a = f RF$. The parameter f could be estimated directly from RF calculations using a radiative transfer code. However, here results from fixed-sea-surface-temperature climate model simulations (e.g. Andrews et al., 2010; Kvalevåg et al., 2103) are used; these have the advantage that they include the impact on f of rapid adjustments of, for example, clouds. A disadvantage is that the results of such experiments are noisier, because of model internal variability, which can be particularly important for small forcings.

The second component of ΔR_d is due to the temperature change resulting from the RF, which leads to an increased emission of longwave radiation. This increase in emission is modified by feedbacks involving other radiatively-important components such as water vapour and clouds (e.g. Takahashi, 2009; Previdi, 2010). Climate model simulations indicate that this component of ΔR_d varies approximately linearly with changes in global-mean surface temperature ΔT_s (e.g. Lambert and Webb, 2008; Previdi, 2010; O’Gorman et al., 2012). These papers also indicate that while generally a smaller term, ΔSH has a similar dependency on ΔT_s (although Ming et al. (2010) have shown that ΔSH can be more important in the case of black carbon changes in the boundary layer).

Hence it is convenient to combine the feedback-related changes in R_d and SH in Eq. (2) into a single term dependent on ΔT_s and separate out the RF term. Equation (2) then becomes, in precipitation units of mm day^{-1} ,

$$\Delta P = 0.034(k\Delta T_s - f\text{RF}). \quad (3)$$

Thorpe and Andrews (2014) show that this formulation does a reasonable job of simulating the precipitation changes from a large number of climate models. We will refer to the $k\Delta T_s$ term as the “ T -term” and the $-f\text{RF}$ term as the “RF-term”. The balance between these two terms varies between climate forcing agents; as will be shown, they can act to either reinforce or oppose each other. Hence the same ΔT_s from two different forcing agents can result in a different ΔP .

Note the sign convention here. For the case of a positive RF, since k is positive, the effect of the T -term is to increase R_d as temperature increases – the increased radiative divergence then leads to a requirement for a greater latent heat flux (and hence an increase in precipitation) to maintain the tropospheric energy balance; this term provides the direct link between surface temperature change and precipitation change. If in this same case f (and hence RF_a) is positive, then the RF-term would oppose the T -term (as it would decrease rather than increase the radiative divergence) and act to suppress precipitation. Physically, in this case, there is less “demand” for latent heating to balance the tropospheric energy budget.

As a simple example of the processes, consider the equilibrium response to a doubling of carbon dioxide, and take $k = 2.2 \text{ W m}^{-2} \text{ K}^{-1}$ (consistent with the multi-model means in Previdi, 2010, and Thorpe and Andrews, 2014), $\text{RF}_{2\times\text{CO}_2} = 3.7 \text{ W m}^{-2}$ (Myhre et al., 2013) and $f = 0.8$ (Andrews et al., 2010), the equilibrium precipitation change $\Delta P_{2\times\text{CO}_2}$ (in %, assuming a global-mean precipitation of 2.68 mm day^{-1}), can be written in terms of the equilibrium surface temperature change $\Delta T_{2\times\text{CO}_2}$ as

$$\Delta P_{2\times\text{CO}_2} = 2.79(\Delta T_{2\times\text{CO}_2} - 1.35). \quad (4)$$

Metrics for linking emissions of gases and aerosols to global precipitation changes

K. P. Shine et al.

Title Page

Abstract

Introduction

Conclusions

References

Tables

Figures

◀

▶

◀

▶

Back

Close

Full Screen / Esc

Printer-friendly Version

Interactive Discussion



Metrics for linking emissions of gases and aerosols to global precipitation changes

K. P. Shine et al.

Title Page

Abstract

Introduction

Conclusions

References

Tables

Figures

◀

▶

◀

▶

Back

Close

Full Screen / Esc

Printer-friendly Version

Interactive Discussion



This equation shows that if $\Delta T_{2\times\text{CO}_2} = 1.35 \text{ K}$, which, via $\Delta T_{2\times\text{CO}_2} = \lambda \text{RF}_{2\times\text{CO}_2}$, corresponds to a climate sensitivity λ of $0.36 \text{ K}(\text{Wm}^{-2})^{-1}$, $\Delta P_{2\times\text{CO}_2}$ would be zero. The slope of the line is $2.79 \% \text{ K}^{-1}$. Such an expression fits well the intercept and slope of the linear fit to equilibrium double- CO_2 experiments from a range of climate models found by Allen and Ingram (2002 – their Fig. 2). The departures of individual models from this best fit could originate from differences in any of the values of k , f or $\text{RF}_{2\times\text{CO}_2}$ assumed here. The slope of the line also corresponds to hydrological sensitivity due only to the T -term, and is in good agreement with the multi-model mean derived by Thorpe and Andrews (2014).

Equation (3) can also be written in a more general form for any ΔT_{eq} (and hence RF_{eq}), so that the equilibrium change in precipitation ΔP_{eq} (in %) is given by

$$\Delta P_{\text{eq}} = 1.3\Delta T_{\text{eq}} \left(k - \frac{f}{\lambda} \right). \quad (5)$$

This emphasizes that the offset between the T - and RF -terms depends strongly on λ . Using a mid-range climate sensitivity of $0.8 \text{ K}(\text{Wm}^{-2})^{-1}$, the RF -term for CO_2 offsets about 50 % of the precipitation change that would result from the T -term alone. Considering the IPCC (2013) “likely” range for λ , which is 0.4 to $1.2 \text{ K}(\text{Wm}^{-2})^{-1}$, the RF -term offsets the T -term by about 90 % for low λ and by 30 % at high λ . The overall global-mean equilibrium hydrological sensitivity ($\Delta P_{\text{eq}}/\Delta T_{\text{eq}}$) to CO_2 forcing can be derived from Eq. (5) and varies from about 0.25 to $2 \% \text{ K}^{-1}$ over this range of λ , which can be compared with the value of $2.79 \% \text{ K}^{-1}$ due solely to the T -term.

To relate the understanding encapsulated in Eq. (3) to an emission of a gas or aerosol, we consider first the GPP for a pulse emission of a unit mass of a gas at time $t = 0$ and consider the precipitation change at a time H after the emission. Following convention, we label this the Absolute GPP (AGPP_{p}), which is presented here in units of $\text{mm day}^{-1} \text{ kg}^{-1}$. The GPP relative to a reference gas will be considered in Sect. 4.

Metrics for linking emissions of gases and aerosols to global precipitation changes

K. P. Shine et al.

Title Page

Abstract

Introduction

Conclusions

References

Tables

Figures

◀

▶

◀

▶

Back

Close

Full Screen / Esc

Printer-friendly Version

Interactive Discussion



The T -term in Eq. (3) becomes k times the absolute GTP_P (AGTP_P) (e.g. Shine et al., 2005). Assuming for small perturbations that RF is linear in the concentration of the emitted species, x , and that the perturbation decays exponentially with time constant τ_x , then for a unit emission, the RF-term is given by $-f_x A_x \exp(-H/\tau_x)$, where A_x is the specific RF (in $\text{W m}^{-2} \text{kg}^{-1}$) of the emitted species. Hence the AGPP (in $\text{mm day}^{-1} \text{kg}^{-1}$) is given by

$$\text{AGPP}_P^x(H) = 0.034(k\text{AGTP}_P^x(H) - f_x A_x \exp(-H/\tau_x)). \quad (6)$$

Since a perturbation of CO_2 does not decay following a simple exponential, the calculation of $\text{AGPP}_P^{\text{CO}_2}(H)$ is slightly more involved – see Appendix for more details.

The effect of a sustained emission of a unit mass of gas per year, from time $t = 0$ can also be considered yielding a sustained AGPP (AGPP_S). In this case, the AGTP_S (see Shine et al., 2005) can be used for the T -term and the RF-term is now proportional to the time variation of the perturbation of the species to a step-perturbation (e.g. Fuglestad et al., 2010). The AGPP_S is given by

$$\text{AGPP}_S^x(H) = 0.034(k\text{AGTP}_S^x(H) - f_x A_x \tau_x (1 - \exp(-H/\tau_x))) \quad (7)$$

which can also be expressed as

$$\text{AGPP}_S^x(H) = 0.034(k\text{AGTP}_S^x(H) - f_x \text{AGWP}_P^x(H)). \quad (8)$$

The calculation of $\text{AGPP}_S^{\text{CO}_2}(H)$ is explained in Appendix. Since a sustained emission can be considered to be equivalent to a succession of pulse emissions, the AGPP_S is the integral of the AGPP_P (see e.g. the Appendix of Berntsen et al., 2005). Note that when H is long compared to the time-scale of the climate response (several hundred years in this case – see Appendix) the $\text{AGTP}_S^x(H)$ can be related to the $\text{AGWP}_P^x(H)$ (see e.g. Shine et al., 2005) which would simplify Eq. (8) further.

3 Illustrative values for the Absolute Global Precipitation-change Potential

In this section, illustrative calculations of the AGPP are presented. The calculation of AGTP, and values for gas lifetimes and A_x follows the methodology presented in Myhre et al. (2013) and is described in more detail in Appendix. The AGTP calculation requires a representation of the surface temperature response, which depends on the climate sensitivity and rate of ocean heat uptake. We use the simple impulse-response function in Boucher and Reddy (2008) (as used in Myhre et al. (2013) for GTP calculations). Values of f , which describe the partitioning of the RF between surface and atmosphere are taken from Andrews et al. (2010) – these will likely be quite strongly model dependent, but for the purposes of illustration, they suffice. Some sensitivity tests to the representation of the impulse-response function and f are presented in Sect. 6. The calculations for emissions of methane and nitrous oxide include indirect effects, the most prominent being their impact on ozone. Different values of f should be used for each indirect component, but in the absence of robust assessments for these, the same value of f is used for all indirect components of the CH_4 and N_2O forcing as is used for the direct components.

3.1 Well-mixed greenhouse gases

Figure 1 shows the AGPP_p for emissions of CO_2 , CH_4 and N_2O , for the total and the RF and T terms individually, for a period up to 100 years after the pulse emission. In Andrews et al. (2010), f is larger for CO_2 (0.8) than for methane (0.5) because, for present-day concentrations, the lower opacity of the methane bands means that the surface feels more of the top-of-the-atmosphere forcing than it does for CO_2 . Since N_2O has a similar atmospheric opacity to CH_4 , it is hypothesized that surface–atmosphere partitioning of the RF also behaves in a similar way to CH_4 and so the value of f for N_2O is also taken to be 0.5; further work would be needed to establish this. Hence, from Eq. (3), the degree of offset between the RF- and T -terms is larger for CO_2 than for CH_4 and N_2O .

Metrics for linking emissions of gases and aerosols to global precipitation changes

K. P. Shine et al.

Title Page

Abstract

Introduction

Conclusions

References

Tables

Figures



Back

Close

Full Screen / Esc

Printer-friendly Version

Interactive Discussion



Metrics for linking emissions of gases and aerosols to global precipitation changes

K. P. Shine et al.

Title Page

Abstract

Introduction

Conclusions

References

Tables

Figures

◀

▶

◀

▶

Back

Close

Full Screen / Esc

Printer-friendly Version

Interactive Discussion



Figure 1a for CO_2 illustrates the general behaviour. For a pulse emission, the size of the RF-term is maximised at the time of emission, as this is when the concentration is largest, and then decays as the perturbation decays. The T -term is dictated by the timescale of the response of the surface temperature to the forcing. The characteristic temperature response to a pulse forcing (e.g. Shine et al., 2005) is an initial increase in T , as the thermal inertia of the surface means it takes time to respond to the forcing, reaching a maximum, followed by a decrease in temperature that is controlled by the timescales of both the decay of the pulse and the temperature perturbation. For the first 5 years, the CO_2 precipitation response is negative as the RF-term dominates, after which the T -term dominates, but the total is approximately 50 % of the T -term. The long perturbation timescales mean that the effect on precipitation persists for more than 100 years after an emission, as does the competition between the T - and RF-terms.

N_2O has a lifetime of the order of a century and its AGPP_p (Fig. 1b) is qualitatively similar to CO_2 but the T -term dominates, because f is smaller. As CH_4 is much shorter lived, its behaviour is somewhat different. As the pulse, and the associated RF, has disappeared by about year 40, after this time the AGPP_p is essentially determined by the T -term only.

3.2 Short-lived species

The AGPP is now illustrated for two short-lived species, sulphate and black carbon (BC) aerosols. For both cases, the radiative efficiency and lifetime values from Myhre et al. (2013) are used and given in the Appendix; for these illustration purposes only the sulphate direct effects are included, and the BC values include some aerosol-cloud interaction and surface albedo effects. In terms of the surface–atmosphere partitioning of RF, these are two contrasting cases. For sulphate, the Andrews et al. (2010) model results indicate an f value less than 0.01 in magnitude and so is assumed here to be zero; this indicates that essentially all of the top-of-the-atmosphere forcing reaches the surface. By contrast, Andrews et al. (2010) find that for BC, f is 2.5, so that the RF_a is much greater than RF; the surface forcing is of opposite sign to RF and RF_a as the

surface is deprived of energy, while the atmosphere gains energy. As will be discussed further in Sect. 6, there are considerable uncertainties in these values, especially for BC, where both RF and f depend strongly on the altitude of the BC. Nevertheless, the values used here suffice to illustrate a number of important points.

Figure 2 shows the AGPP_P for both black carbon and sulphate. As both are very short-lived (weeks) compared to the greenhouse gases, their RF-term decays to zero within a year (and hence is not visible on Fig. 2), and it is only the thermal inertia of the climate system that enables them to influence temperature beyond this time period.

An alternative perspective of the effect of sulphate and BC is provided for the sustained-emissions case. In this case, because the BC and sulphate perturbations persist, so too does the influence of the RF-term on precipitation. Figure 3 shows the AGPP_S for CO₂, BC and sulphate. For CO₂, the long-time scales of CO₂ perturbation mean that both the RF term and T term increase throughout the 100 year period shown. At short time-horizons, the RF-term dominates, leading to suppression of global precipitation, but after about 15 years, the T -term starts to dominate, and the AGPP_S becomes positive.

For BC, the impact of the large RF-term is dramatic. It is strongly negative and constant with time (because of the short lifetime), while the T term is positive and increases until the temperature is almost in equilibrium with the RF. This counteracts the impact of the RF term on the total, but the total nevertheless remains negative throughout. For sulphate, because f is assumed to be zero, the total remains equal to the T -term.

4 The GPP relative to CO₂

4.1 Background

One potential application of the GPP is to place the emissions of different species on a common scale, in a similar way to the GWP. The 100 year time-horizon GWP (GWP(100)) is used by the Kyoto Protocol to the United Nations' Framework Con-

Metrics for linking emissions of gases and aerosols to global precipitation changes

K. P. Shine et al.

Title Page

Abstract

Introduction

Conclusions

References

Tables

Figures

◀

▶

◀

▶

Back

Close

Full Screen / Esc

Printer-friendly Version

Interactive Discussion



Metrics for linking emissions of gases and aerosols to global precipitation changes

K. P. Shine et al.

Title Page

Abstract

Introduction

Conclusions

References

Tables

Figures

◀

▶

◀

▶

Back

Close

Full Screen / Esc

Printer-friendly Version

Interactive Discussion



vention on Climate Change to place emissions of many relatively well-mixed non-CO₂ greenhouse gases on a so-called “CO₂-equivalent scale”; this is necessary for the type of multi-gas treaty that the Kyoto Protocol represents. Metrics such as the GWP can also be used in life-cycle assessment and carbon footprint studies, for assessing possible mitigation strategies, for example in particular economic sectors, and can extend beyond the gases included in the Kyoto Protocol (see e.g. Fuglestvedt et al., 2010; Deuber et al., 2014).

The GWP characterises the RF in response to a pulse emission of a substance, integrated over some specified time horizon. It is normally expressed relative to the same quantity for an equal-mass emission of CO₂. The GWP has enabled the multi-gas operation of the Kyoto Protocol but has also been the subject of criticism for some applications (e.g. Myhre et al. (2013), Pierrehumbert (2014) and references therein). This is partly because the use of time-integrated RF does not clearly relate to an impact of climate change (such as temperature change) and also because it contains value judgements (particularly the choice of time horizon) that cannot be rigorously justified for any particular application (Myhre et al., 2013).

Metrics that extend beyond time-integrated forcing have also been proposed. The GTP (e.g. Shine et al., 2007; Myhre et al., 2013) characterises the global-mean surface temperature change at some time after an emission. It may be more applicable to policies that aim to restrict temperature change below a given target level. The GTP is also subject to criticism and the need for value judgements when choosing time horizons (Myhre et al., 2013). Nevertheless the GTP (and its variants, such as the mean global temperature-change potential – e.g. Gillett and Matthews, 2010; Deuber et al., 2014 – and integrated temperature potential – e.g. Peters et al., 2011; Azar and Johansson, 2012) do at least extend to a parameter (temperature change) more obviously related to a climate change impact. Sterner et al. (2014) recently presented a metric for sea-level rise. Metrics can be extended to the economic effects of an emission (for example the Global Cost Potential and Global Damage Potential), by relating the metrics to costs and damages (e.g. Johansson, 2012) and in certain restrictive

Metrics for linking emissions of gases and aerosols to global precipitation changes

K. P. Shine et al.

Title Page

Abstract

Introduction

Conclusions

References

Tables

Figures

◀

▶

◀

▶

Back

Close

Full Screen / Esc

Printer-friendly Version

Interactive Discussion



cases these can be shown to have equivalence to physically-based metrics such as the GWP and GTP (e.g. Tol et al., 2012). One difficulty in such approaches is that the economic damage has to be represented in a highly-idealised form, as some simple function of, for example, temperature change. Conventional physical metrics can also be judged in an economic context (e.g. Reisinger et al., 2012; Strefler et al., 2014).

Here the $AGPP_P$ and $AGPP_S$ are used to calculate the GPP_P and GPP_S relative to a reference gas, and following the common practice for GWP and GTP, CO_2 is used as that reference gas here, although difficulties with this choice will be noted. The GPP_P , relative to an equal mass emission of CO_2 , is then be given by

$$GPP_P^x(H) = \frac{AGPP_P^x(H)}{AGPP_P^{CO_2}(H)} \quad (9)$$

with a similar expression for the GPP_S .

4.2 Well-mixed greenhouse gases

Figure 4 shows the GPP_P for N_2O and CH_4 ; for comparison, the GTP_P is also shown. Note that the plots start at $H = 20$ years, as the time at which the different $AGPP_P$'s cross the zero axis differs slightly amongst the gases, and this results in a singularity in Eq. (9). For N_2O , the GPP_P is at least 300 times greater than CO_2 on all timescales shown, and, per unit emission, is more than 40 % more effective at changing precipitation than temperature (as given by the GTP_P), compared to CO_2 . This is because the RF term is less effective at muting the T -term for N_2O 's GPP_P than is the case for CO_2 . For CH_4 the difference between the GPP_P and GTP_P is most marked in an absolute sense at shorter time horizons, when the GPP_P of methane is affected most by the RF-term; the GPP_P and the absolute difference with the GTP decline at longer time scales when it is entirely due to the difference between the $AGTP_P$ and $AGPP_P$ for CO_2 .

Metrics for linking emissions of gases and aerosols to global precipitation changes

K. P. Shine et al.

Title Page

Abstract

Introduction

Conclusions

References

Tables

Figures

◀

▶

◀

▶

Back

Close

Full Screen / Esc

Printer-friendly Version

Interactive Discussion



Table 1 presents the values of the GWP_P , GTP_P and GPP_P for H of 20 and 100 years; these time horizons are chosen for illustrative purposes, rather than being indicative that they have special significance, except insofar as 100 years is used for the GWP within the Kyoto Protocol (Myhre et al., 2013). For CH_4 , the $GPP_P(20)$ is 50 % larger than the $GWP_P(20)$ and almost double the $GTP_P(20)$ mostly because of the larger effect of the RF-term on the GPP_P for CO_2 . The time-integrated nature of the GWP_P means that it is much higher than the GTP_P and GPP_P at 100 years, while the GPP_P remains about double the GTP_P . The effectiveness of N_2O at changing precipitation (relative to CO_2) is 40–50 % higher than the GWP_P and GTP_P at both values of H , again because of the larger effect of the RF-term on the GPP_P for CO_2 .

4.3 Short-lived species

Figure 5 shows the GPP_P and GTP_P for black carbon and sulphate. As noted in Sect. 3.2, the radical difference in their values of f (2.5 for black carbon, 0 for sulphate) has no impact on the AGPP for BC and sulphate beyond very short timescales. Because of this, in Fig. 5, the only difference between the GPP_P and GTP_P comes from the influence of the RF-term on the $AGPP_P^{CO_2}$, and on an equal emissions basis both short-lived species are, relative to CO_2 , more effective at changing precipitation than temperature – this is also shown in Table 1.

Figure 6 shows the GPP_S , comparing it with the GTP_S . For sulphate, the difference between the GPP_S and GTP_S originates entirely from the effect of the RF-term on $AGPP_S^{CO_2}$, because of the assumption that f is zero, but they differ dramatically for black carbon – whilst both BC and CO_2 cause a warming, so that the GTP_S is positive, their impact on precipitation is opposite, and the BC GPP_S is negative.

Table 2 presents values of the GTP_S and GPP_S for $H = 20$ and 100 years, including the values for CH_4 and N_2O for completeness. The GPP_S values at 20 years are particularly influenced by the fact that the $AGPP_S$ for CO_2 is relatively small at this time, due to the strong cancellation between the T and RF terms. At both values of H , the GPP_S

values are higher in magnitude than the corresponding GTP_S values for all non- CO_2 components.

5 Precipitation response to more realistic emissions

To illustrate a further usage of the $AGPP_P$ and $AGPP_S$, Figs. 7 and 8 apply them to 2008 emissions, to examine the consequences of the emissions of the 5 example species on precipitation. Figure 8.33 of Myhre et al. (2013) presents a similar calculation applying the $AGTP_P$ and shows that the 5 species used here are the dominant emissions for determining temperature change; hence it was felt useful to present the total effect of the 5 emissions in the figures as well. Emissions are taken from Table 8.SM.18 of Myhre et al. (2013) and reproduced in Table A1. For reference, the corresponding values using the $AGTP_P$ and $AGTP_S$ are also shown.

Figure 7 shows the impact of the 2008 emissions, emitted as a single pulse, on global precipitation and temperature change in subsequent years. While the emissions of CH_4 , sulphate and BC are 2 to 4 orders of magnitude smaller than those of CO_2 , in the early years after the emission, their effects are competitive with CO_2 because of the size of the GPP_P and GTP_P ; despite N_2O 's large GPP_P , its emission are small enough that its absolute contribution remains low throughout. Because of the differing compensations between the T - and RF-terms for CO_2 and CH_4 , their relative importance differs quite significantly between the precipitation and temperature calculations. Methane's contribution to precipitation change is less negative or more positive than that of CO_2 until about 20 years; it exceeds the CO_2 contribution by a factor of 2 at about 10 years, and remains 25 % of the CO_2 effect even at 50 years. For temperature, the contributions are approximately the same until 10 years, after which the CO_2 contribution dominates, being about 7 times larger by 50 years. For the two aerosol components, the GPP_P is unaffected by the RF-term (see Sect. 3) but their importance for precipitation relative to CO_2 is enhanced, because the RF-term acts to suppress the

Metrics for linking emissions of gases and aerosols to global precipitation changes

K. P. Shine et al.

Title Page

Abstract

Introduction

Conclusions

References

Tables

Figures

◀

▶

◀

▶

Back

Close

Full Screen / Esc

Printer-friendly Version

Interactive Discussion



effect of CO₂ on precipitation change. Thus, for example, the BC effect on precipitation is larger than CO₂ out to year 10, compared to year 4 for temperature.

Figure 8 shows the effect of assuming sustained emissions at 2008 levels. Although not a plausible future scenario (since, for example, emissions of greenhouse gases are at present continuing to rise) it provides a useful baseline experiment to assess the relative roles of current emissions on future global changes in temperature and precipitation. As expected from the AGPP_S values, the role of the short-lived species differs considerably from the pulse case, as the RF-term remains active – in the case of precipitation, BC's effect is now negative throughout. Until about 30 years, the net effect of all 5 emissions is a reduction of precipitation, after which the warming due to CH₄ and CO₂ is sufficient for their *T*-terms to overwhelm the reduction caused by sulphate (due to its *T*-term) and BC (due to its RF-term). This near-term reduction of precipitation is also seen in the results of Allan et al. (2014), where the precipitation changes are driven directly by forcings and temperatures (rather than by emissions, as is the case here). By contrast, the temperature effect is positive after year 1. Perhaps most marked is the role of CH₄. It is the dominant driver of positive precipitation change until about year 50 and even after 100 years its effect is about 50% of that due to CO₂. By contrast, for temperature, the CO₂ effect is greatest after 15 years and 3 times larger by 100 years. Figure 8 also illustrates the extent to which the sulphate and BC emissions are opposing the precipitation increase due to the greenhouse gases, at large values of *H*; this component would be relatively quickly responsive to any changes in emissions.

While these are clearly idealised applications of uncertain metrics, they nevertheless illustrate their potential utility for assessing the relative importance over time of different emissions on global precipitation change. The approach could be extended to past or possible future emission profiles, by convolving the time-dependent emissions with the GTP_P and GPP_S values.

Metrics for linking emissions of gases and aerosols to global precipitation changes

K. P. Shine et al.

Title Page

Abstract

Introduction

Conclusions

References

Tables

Figures



Back

Close

Full Screen / Esc

Printer-friendly Version

Interactive Discussion



6 Sensitivities and uncertainties

There are a wide range of uncertainties and sensitivities in the calculation of metrics such as the GWP, GTP and GPP, such as assumptions about the background state, that can affect A_x and τ_x , and assumptions about the impulse-response function for CO_2 (see e.g. Fuglestvedt et al., 2010; Myhre et al., 2013). Two particular sensitivities are explored here. First, the impulse-response model for surface temperature change used here (see beginning of Sect. 3) is a fit to output from experiments with one particular climate model with its own particular climate sensitivity. Oliv   et al. (2012) present similar fits derived from 17 different climate models, or model variants, from the Coupled Model Intercomparison Project 3 database – the fits for the “gradual scenarios” shown in Table 5 of Oliv   et al. (2012) are used here, along with the Boucher and Reddy (2008) fit used in Sect. 3. These fits are for models with a wide range of climate sensitivities (0.49 to $1.06 \text{ K (W m}^{-2}\text{)}^{-1}$) and the timescales of the fitted modes vary significantly amongst the models. Oliv   and Peters (2013) used these fits to explore the sensitivity of the GTP calculations. Figure 9 shows the mean and SD of the GTP and GPP values for both pulse and sustained emissions derived using these 18 different representations.

Considering first the pulse values for the absolute metrics for CO_2 (Fig. 9a) it can be seen that the AGTP_P is only moderately sensitive (with a coefficient of variation (cv) of about 20 %) to model choice. By contrast for AGPP_P (20), the cv is about 60 % and even for the AGPP_P (100) it is about 40 %. This is because the T -term is highly sensitive to the model choice, whilst the RF -term is independent, and hence the degree of compensation between these two terms varies amongst the impulse-response models. The GTP_P sensitivity is greatest for short-lived species and this uncertainty is amplified for the GPP_P , by up to a factor of 2 in the case of the GPP_P (100) for sulphate (Fig. 9d). By contrast, for the longer-lived species the uncertainty in the GTP_P and GPP_P differ greatly – for N_2O (Fig. 9c), the cv for GTP_P values is only a percent or so, but is typically 40 % for the GPP_P , as both the numerator and denominator in the GPP_P expression

Metrics for linking emissions of gases and aerosols to global precipitation changes

K. P. Shine et al.

Title Page

Abstract

Introduction

Conclusions

References

Tables

Figures

◀

▶

◀

▶

Back

Close

Full Screen / Esc

Printer-friendly Version

Interactive Discussion



are impacted by compensations in the T - and RF-terms to different degrees at different times.

The GPP_S is more sensitive because even the sign of the $AGPP_S^{CO_2}$ is not well constrained at 20 years (Fig. 9a). Roughly half of the impulse-response models yield a positive value and half a negative one, with two very close to zero, because of the differing degrees of compensation between the T - and RF-terms amongst the impulse response functions (see Sect. 2). The value of H at which the $AGPP_S^{CO_2}$ is zero varies from 11 to 61 years amongst the different temperature impulse response models. (For comparison, for the $AGPP_P^{CO_2}$, the corresponding range is 4 to 13 years.) In these circumstances, it becomes essentially pointless to compare the GPP_S values as they vary wildly from model to model (from $-18\,000$ to $24\,000$ for the $GPP_S(20)$ for N_2O) and for this reason the absolute GPP_S (i.e. $AGPP_S$) values are presented in Fig. 9. Even the $AGPP_S^{CO_2}(100)$ values vary by over an order of magnitude across the 18 representations. In general, the uncertainty in the $AGPP_S$ exceed those in the GPP_S ; this is most marked in the case of N_2O , where the GPP_S is almost insensitive to the choice of impulse-response function, as the effect of this choice on the $AGPP_S$ for CO_2 and N_2O is almost the same.

The second sensitivity is the values of f used in the calculations. The values presented by Andrews et al. (2010) are replaced by those from Kvalevåg et al. (2013). For some forcing mechanisms Kvalevåg et al. (2013) derived f values for a range of sizes of forcing perturbations. In all case, the values from the larger forcing perturbations are used here as these give a clearer signal for the value of f . Compared to Andrews et al. (2010), for CO_2 f reduces from 0.8 to 0.6, for CH_4 (and, it is assumed for N_2O) it decreases from 0.5 to 0.3 and for sulphate it decreases from zero to -0.4 (which implies much greater atmospheric absorption associated with sulphate forcing than found by Andrews et al., 2010). For BC, Kvalevåg et al. (2013) present a range of values, appropriate for perturbations at different altitudes – for example they find a value of f of 6.2 (for 10 times the model-derived vertical profile of BC in response to present-day emissions) and 13 (when 10 times the present-day burden is placed

ESDD

6, 719–760, 2015

Metrics for linking emissions of gases and aerosols to global precipitation changes

K. P. Shine et al.

Title Page

Abstract

Introduction

Conclusions

References

Tables

Figures



Back

Close

Full Screen / Esc

Printer-friendly Version

Interactive Discussion



entirely at 550 hPa); these can be compared to the Andrews et al. (2010) value of 2.5. The difference results mostly from the semi-direct effect of BC and clouds; when BC is entirely placed at certain pressures (750 and 650 hPa), Kvalevåg et al.'s (2013) results indicate that f is particularly poorly constrained, because RF is close to zero, while RF_{atm} is large and positive.

Table 3 presents results for the GPP_P and GPP_S , which should be compared with the appropriate columns in Tables 1 and 2 (the GWP , GTP_P and GTP_S values are unchanged when f is changed). For the GPP_P for CH_4 and N_2O , the effect of changing to the Kvalevåg et al. (2013) f values are rather modest (10–20 %) because changes in the numerator and denominator of Eq. (9) compensate to some extent. For BC and sulphate, changes are entirely dependent on the change in $AGPP_P^C$, as the change in f factor has less influence (see Sect. 3.2) and changes are correspondingly larger (20–30 %).

For the GPP_S , the $AGPP_S^{CO_2}(20)$ is rather sensitive to the change in f because of the degree of compensation between the T - and RF-terms, and increases by more than a factor of 2. This is the dominant reason why the $GPP_S(20)$ for N_2O and CH_4 decrease by about a factor of 2. The changes at 100 years are much smaller, nearer 10 %. The $AGPP_S$ for the short-lived species are, unlike the $AGPP_P$, now affected by the change in f . Table 5 shows the effect on the sulphate $GPP_S(20)$ to be about a factor of 2, while the $GPP_S(100)$ is little affected. By contrast, the GPP_S for black carbon at both time horizons depends significantly on the altitude of the black carbon perturbation.

7 Discussion and conclusions

This paper has used a simple, but demonstrably useful, conceptual model of the drivers of global-mean precipitation change in response to the imposition of a radiative forcing, to relate precipitation change directly to emissions. The GPP_P and GPP_S metrics illustrate the interplay between the two drivers (the atmospheric component of the ra-

Metrics for linking emissions of gases and aerosols to global precipitation changes

K. P. Shine et al.

Title Page

Abstract

Introduction

Conclusions

References

Tables

Figures

◀

▶

◀

▶

Back

Close

Full Screen / Esc

Printer-friendly Version

Interactive Discussion



diative forcing, and the surface temperature change) for different forcings, at different time horizons, and for both pulse and sustained emissions.

It has been shown that relative to CO₂, the pulse and sustained GPP values for the non-CO₂ species examined here are larger than the corresponding GTP values, because the CO₂ GPP is the sum of two quite strongly opposing terms. Further, for black carbon emissions, while they act to warm the climate system, they also act to reduce global-mean precipitation; while this has been clear from the modelling literature for some time, the present work shows how the perspective is different for pulse and sustained emissions. The reduction of precipitation is driven entirely by the radiative forcing component and since, for pulse emissions of short-lived species this falls away on time scales of weeks, it is only apparent on longer time-scales for the sustained perspective. This is an example of how the perturbation design can have a large impact on the calculated response.

The evaluation of precipitation metrics assumes that the parameters required for the simple conceptual model are available, and in particular the partitioning of radiative forcing between surface and atmosphere. Only a rather limited number of model studies of this partitioning are currently available, and there are significant differences amongst these and particular sensitivity to the altitude of absorbing aerosol (e.g. Ming et al., 2010; Kvalevåg et al., 2013). The ongoing Precipitation Driver Response Model Intercomparison Project (PDRMIP) (<http://cicero.uio.no/PDRMIP/>) should provide important information of the degree of robustness of this partitioning amongst a range of climate models for a number of radiative forcing mechanisms, but clearly further studies, for a wider range of forcing agents are needed.

It is not suggested that the new metrics could replace conventional emissions metrics such as the GWP and GTP in climate policies or emission trading context, but they do provide a useful additional perspective for assessing effects of emissions; they particularly help to emphasise where the impact on precipitation differs significantly from that on temperature or forcing. One difficulty in its application is that conventional metrics generally use CO₂ as a reference gas. For precipitation change, the forcing and sur-

Metrics for linking emissions of gases and aerosols to global precipitation changes

K. P. Shine et al.

Title Page

Abstract

Introduction

Conclusions

References

Tables

Figures

◀

▶

◀

▶

Back

Close

Full Screen / Esc

Printer-friendly Version

Interactive Discussion



Metrics for linking emissions of gases and aerosols to global precipitation changes

K. P. Shine et al.

Title Page

Abstract

Introduction

Conclusions

References

Tables

Figures

◀

▶

◀

▶

Back

Close

Full Screen / Esc

Printer-friendly Version

Interactive Discussion



face temperature components oppose each other, which means that the effect of CO₂ emissions on precipitation can be zero (at least in the global-mean) at short time horizons for both pulse and sustained emissions. This is clearly undesirable for a reference gas, and it has also been shown that the timing of this zero point is rather sensitive to the particular parameters used in its calculation. Hence absolute metrics may be more instructive. By applying the absolute metrics to a specific illustrative case (emissions in 2008, either as a pulse, or sustained indefinitely) the importance of methane in influencing the global-mean precipitation change is highlighted – using the default model parameters here, in the sustained 2008 emissions case, the precipitation change from methane exceeds that from CO₂ for about 50 years; by contrast, for the temperature case, the effect of CO₂ emissions are almost immediately at least comparable to, or stronger than, methane.

It has been stressed that use of global-mean precipitation change as a measure of impact has difficulties, because predicted future changes differ in sign between regions – the global-mean is a small residual of these opposing more localised changes and hence it only gives rather general guidance on the effect of different drivers on the changing hydrological cycle. Nevertheless, as noted in the Introduction, some of that regional variability can be understood as a generic response to temperature change. The approach here could be enhanced to a more regional level of response by either using a simple pattern-scaling approach (whereby the pattern of predicted precipitation change scales with the global-mean) or, better, to derive a regional variation that accounts for the different effects of the forcing and temperature response on precipitation change (Good et al., 2012). The patterns emerging from such an approach would likely depend significantly on which climate model was used to derive them. In addition, such patterns would be needed for all the primary forcing agents.

For short-lived emissions, it is known that even global-mean metrics such as the GWP and GTP depend on the emission location (e.g. Fuglestvedt et al., 2010) – this will also be true for the precipitation metrics. Metrics can also be posed in terms of the regional response to regional emissions (see e.g. Collins et al., 2013 who employed

Metrics for linking emissions of gases and aerosols to global precipitation changes

K. P. Shine et al.

Title Page

Abstract

Introduction

Conclusions

References

Tables

Figures

◀

▶

◀

▶

Back

Close

Full Screen / Esc

Printer-friendly Version

Interactive Discussion



the Regional Temperature Potential proposed by Shindell (2012) whereby a matrix is produced that characterises the effect of RFs in a set of given regions on the temperature change in a set of given regions). Regional versions of the GPP could also be derived, and it is likely that the regional variation of the response would be even larger for precipitation change than temperature change.

In spite of the difficulties in quantifying the precipitation metrics given present knowledge of the driving parameters, the framework presented here adds a useful extra dimension to simple tools that are currently available for assessing the impact of emissions of different gases and particulates.

Appendix

The impulse response function, $R(t)$, for a pulse emission of CO_2 is assumed to be of the form

$$R(t) = a_0 + \sum_j a_j \exp\left(-\frac{t}{\alpha_j}\right) \quad (\text{A1})$$

where the parameters are the same as those in Myhre et al. (2013), with $a_0 = 0.2173$, $a_1 = 0.2240$, $a_2 = 0.2824$, $a_4 = 0.2763$ and $\alpha_1 = 394.4$, $\alpha_2 = 36.54$ and $\alpha_3 = 4.304$ years.

The impulse response function for global-mean surface temperature is taken from Boucher and Reddy (2008) and is of the form

$$R(t) = \sum_i \frac{c_i}{d_i} \exp\left(-\frac{t}{d_i}\right) \quad (\text{A2})$$

with $c_1 = 0.631$, $c_2 = 0.429 \text{ K}(\text{W m}^{-2})^{-1}$ and $d_1 = 8.4$ and $d_2 = 409.5$ years. The equilibrium climate sensitivity for this function is $1.06 \text{ K}(\text{W m}^{-2})^{-1}$, equivalent to an equilibrium surface temperature change for a doubling of CO_2 of about 3.9 K.

Using Eq. (A2), the AGTP_P for a species with a specific RF A_x and a lifetime τ_x is given by

$$AGTP_P^x(t) = A_x \tau_x \sum_{i=1}^2 \frac{c_i}{\tau_x - d_i} (\exp(-t/\tau_x) - \exp(-t/d_i)). \quad (A3)$$

This equation does not apply in the case where $\tau_x = d_i$; the appropriate expression is given in Shine et al. (2005) for this case, which has to be modified for the two-term form of Eq. (A2).

For the case of CO₂, where the decay of a pulse is given by Eq. (A1), the AGTP_P is given by

$$AGTP_P^{CO_2}(t) = A_{CO_2} \left[a_0 \sum_{i=1}^2 c_i \left(1 - \exp\left(-\frac{t}{d_i}\right) \right) + \sum_{i=1}^2 c_i \sum_{j=1}^3 \frac{a_j \alpha_j}{\alpha_j - d_i} (\exp(-t/\alpha_j) - \exp(-t/d_i)) \right]. \quad (A4)$$

For the case of CO₂, the exponential in the second term on the right-hand side of Eq. (6) is replaced by Eq. (A1) for the calculation of AGPP_P^{CO₂}(H).

The GTP_S for non-CO₂ species is given by

$$AGTP_S^x(t) = A_x \tau_x \left[\sum_{i=1}^2 c_i \left(1 - \exp(-t/d_i) - \frac{\tau_x}{\tau_x - d_i} (\exp(-t/\tau_x) - \exp(-t/d_i)) \right) \right] \quad (A5)$$

and again the case where $\tau_i = d_i$ is given in Shine et al. (2005), which has to be modified for the two-term form of Eq. (A2).

Metrics for linking emissions of gases and aerosols to global precipitation changes

K. P. Shine et al.

Title Page	
Abstract	Introduction
Conclusions	References
Tables	Figures
◀	▶
◀	▶
Back	Close
Full Screen / Esc	
Printer-friendly Version	
Interactive Discussion	



Metrics for linking emissions of gases and aerosols to global precipitation changes

K. P. Shine et al.

Title Page

Abstract

Introduction

Conclusions

References

Tables

Figures

◀

▶

◀

▶

Back

Close

Full Screen / Esc

Printer-friendly Version

Interactive Discussion



For CO₂ the AGTP_S is given by

$$\text{AGTP}_S^{\text{CO}_2}(t) = \sum_{i=1}^2 A_{\text{CO}_2} c_i \left[a_o(t - d_i(1 - \exp(-t/d_i))) + \sum_{j=1}^3 \alpha_j a_j \left(1 - \exp(-t/d_j) - \frac{\alpha_j}{\alpha_j - d_j} (\exp(-t/\alpha_j) - \exp(-t/d_j)) \right) \right]. \quad (\text{A6})$$

The AGWP_P^{CO₂}, which is required in the second term on the right hand side of Eq. (7) in the case of CO₂, is given by

$$\text{AGWP}_P^{\text{CO}_2}(t) = A_{\text{CO}_2} \left(a_o H + \sum_{j=1}^3 a_j \alpha_j \left(1 - \exp\left(-\frac{t}{\alpha_j}\right) \right) \right). \quad (\text{A7})$$

The parameters used for the 5 different species employed here are presented in Table A1.

Author contributions. K. P. Shine conceived the idea of the emissions metrics for precipitation, through conversations with R. P. Allan, performed the calculations and led the writing. R. P. Allan, W. J. Collins and J. S. Fuglestedt provided major critical input to the drafts, including ideas on adjusting the main emphasis of the paper and on possible applications of the metrics.

Acknowledgements. We acknowledge funding from the European Commission, under the ECLIPSE (Evaluating the Climate and Air Quality Impacts of Short-Lived Pollutants) Project (Grant Agreement 282 688) and thank other ECLIPSE partners for their encouragement and input to this work.

References

- Allan, R. P., Liu, C. L., Zahn, M., Lavers, D. A., Koukouvagias, E., and Bodas-Salcedo, A.: Physically consistent responses of the global atmospheric hydrological cycle in models and observations, *Surv. Geophys.*, 35, 533–552, doi:10.1007/s10712-012-9213-z, 2014.
- 5 Allen, M. R. and Ingram, W. J.: Constraints on future changes in climate and the hydrologic cycle, *Nature*, 419, 224–232, doi:10.1038/nature01092, 2002.
- Andrews, T., Forster, P. M., Boucher, O., Bellouin, N., and Jones, A.: Precipitation, radiative forcing and global temperature change, *Geophys. Res. Lett.*, 37, L14701, doi:10.1029/2010gl043991, 2010.
- 10 Azar, C. and Johansson, D. J. A.: On the relationship between metrics to compare greenhouse gases – the case of IGTP, GWP and SGTP, *Earth Syst. Dynam.*, 3, 139–147, doi:10.5194/esd-3-139-2012, 2012.
- Berntsen, T., Fuglestedt, J., Joshi, M., Shine, K., Stuber, N., Ponater, M., Sausen, R., Hauglustaine, D., and Li, L.: Response of climate to regional emissions of ozone precursors: sensitivities and warming potentials, *Tellus B*, 57, 283–304, doi:10.1111/j.1600-0889.2005.00152.x, 2005.
- 15 Boucher, O. and Reddy, M. S.: Climate trade-off between black carbon and carbon dioxide emissions, *Energ. Policy*, 36, 193–200, doi:10.1016/j.enpol.2007.08.039, 2008.
- Collins, W. J., Fry, M. M., Yu, H., Fuglestedt, J. S., Shindell, D. T., and West, J. J.: Global and regional temperature-change potentials for near-term climate forcers, *Atmos. Chem. Phys.*, 20 13, 2471–2485, doi:10.5194/acp-13-2471-2013, 2013.
- Deuber, O., Luderer, G., and Sausen, R.: CO₂ equivalences for short-lived climate forcers, *Climatic Change*, 122, 651–664, doi:10.1007/s10584-013-1014-y, 2014.
- Fuglestedt, J. S., Shine, K. P., Berntsen, T., Cook, J., Lee, D. S., Stenke, A., Skeie, R. B., 25 Velders, G. J. M., and Waitz, I. A.: Transport impacts on atmosphere and climate: metrics, *Atmos. Environ.*, 44, 4648–4677, doi:10.1016/j.atmosenv.2009.04.044, 2010.
- Gillett, N. P. and Matthews, H. D.: Accounting for carbon cycle feedbacks in a comparison of the global warming effects of greenhouse gases, *Environ. Res. Lett.*, 5, 034011, doi:10.1088/1748-9326/5/3/034011, 2010.
- 30 Good, P., Ingram, W., Lambert, F. H., Lowe, J. A., Gregory, J. M., Webb, M. J., Ringer, M. A., and Wu, P. L.: A step-response approach for predicting and understanding non-linear precipitation changes, *Clim. Dynam.*, 39, 2789–2803, doi:10.1007/s00382-012-1571-1, 2012.

Metrics for linking emissions of gases and aerosols to global precipitation changes

K. P. Shine et al.

Title Page

Abstract

Introduction

Conclusions

References

Tables

Figures

◀

▶

◀

▶

Back

Close

Full Screen / Esc

Printer-friendly Version

Interactive Discussion



Metrics for linking emissions of gases and aerosols to global precipitation changes

K. P. Shine et al.

Title Page

Abstract

Introduction

Conclusions

References

Tables

Figures

◀

▶

◀

▶

Back

Close

Full Screen / Esc

Printer-friendly Version

Interactive Discussion



- Held, I. M. and Soden, B. J.: Robust responses of the hydrological cycle to global warming, *J. Climate*, 19, 5686–5699, doi:10.1175/jcli3990.1, 2006.
- Huffman, G. J., Adler, R. F., Bolvin, D. T., and Gu, G. J.: Improving the global precipitation record: GPCP version 2.1, *Geophys. Res. Lett.*, 36, L17808, doi:10.1029/2009gl040000, 2009.
- 5 IPCC: Climate Change 2013: The Physical Science Basis, Contribution of Working Group I to the Fifth Assessment Report of the Intergovernmental Panel on Climate Change, Cambridge University Press, Cambridge, UK and New York, NY, USA, 1535 pp., 2013.
- Johansson, D. J. A.: Economics- and physical-based metrics for comparing greenhouse gases, *Climatic Change*, 110, 123–141, doi:10.1007/s10584-011-0072-2, 2012.
- 10 Knutti, R. and Sedlacek, J.: Robustness and uncertainties in the new CMIP5 climate model projections, *Nat. Clim. Change*, 3, 369–373, doi:10.1038/nclimate1716, 2013.
- Kvalevag, M. M., Samset, B. H., and Myhre, G.: Hydrological sensitivity to greenhouse gases and aerosols in a global climate model, *Geophys. Res. Lett.*, 40, 1432–1438, doi:10.1002/grl.50318, 2013.
- 15 Lambert, F. H. and Webb, M. J.: Dependency of global mean precipitation on surface temperature, *Geophys. Res. Lett.*, 35, L16706, doi:10.1029/2008gl034838, 2008.
- Liu, C. L. and Allan, R. P.: Observed and simulated precipitation responses in wet and dry regions 1850–2100, *Environ. Res. Lett.*, 8, 034002, doi:10.1088/1748-9326/8/3/034002, 2013.
- 20 Ming, Y., Ramaswamy, V., and Persad, G.: Two opposing effects of absorbing aerosols on global-mean precipitation, *Geophys. Res. Lett.*, 37, L13701, doi:10.1029/2010gl042895, 2010.
- Mitchell, J. F. B., Wilson, C. A., and Cunningham, W. M.: On CO₂ climate sensitivity and model dependence of results, *Q. J. Roy. Meteorol. Soc.*, 113, 293–322, doi:10.1002/qj.49711347517, 1987.
- 25 Myhre, G., Shindell, D., Breion, F.-M., Collins, W., Fuglestedt, J., Huang, J., Koch, D., Lamarque, J.-F., Lee, D., Mendoza, B., Nakajima, T., Robock, A., Stephens, G., Takemura, T., and Zhang, H.: Anthropogenic and Natural Radiative Forcing, in: *Climate Change 2013: The Physical Science Basis, Contribution of Working Group I to the Fifth Assessment Report of the Intergovernmental Panel on Climate Change*, edited by: Stocker, T. F., Qin, D., Plattner, G. K., Tignor, M., Allen, S. K., Boschung, J., Nauels, A., Xia, Y., Bex, V., and Midgley, P. M., Cambridge University Press, Cambridge, UK and New York, NY, USA, 659–740, 30 2013.

Metrics for linking emissions of gases and aerosols to global precipitation changes

K. P. Shine et al.

Title Page

Abstract

Introduction

Conclusions

References

Tables

Figures

◀

▶

◀

▶

Back

Close

Full Screen / Esc

Printer-friendly Version

Interactive Discussion



O’Gorman, P. A., Allan, R. P., Byrne, M. P., and Previdi, M.: Energetic constraints on precipitation under climate change, *Surv. Geophys.*, 33, 585–608, doi:10.1007/s10712-011-9159-6, 2012.

5 Olivie, D. J. L. and Peters, G. P.: Variation in emission metrics due to variation in CO₂ and temperature impulse response functions, *Earth Syst. Dynam.*, 4, 267–286, doi:10.5194/esd-4-267-2013, 2013.

Olivie, D. J. L., Peters, G. P., and Saint-Martin, D.: Atmosphere response time scales estimated from AOGCM Experiments, *J. Climate*, 25, 7956–7972, doi:10.1175/jcli-d-11-00475.1, 2012.

10 Peters, G. P., Aamaas, B., Berntsen, T., and Fuglestvedt, J. S.: The integrated global temperature change potential (iGTP) and relationships between emission metrics, *Environ. Res. Lett.*, 6, 044021, doi:10.1088/1748-9326/6/4/044021, 2011.

Pierrehumbert, R. T.: Short-lived climate pollution, *Annu. Rev. Earth Pl. Sc.*, 42, 341–379, doi:10.1146/annurev-earth-060313-054843, 2014.

15 Previdi, M.: Radiative feedbacks on global precipitation, *Environ. Res. Lett.*, 5, 025211, doi:10.1088/1748-9326/5/2/025211, 2010.

Reisinger, A., Havlik, P., Riahi, K., van Vliet, O., Obersteiner, M., and Herrero, M.: Implications of alternative metrics for global mitigation costs and greenhouse gas emissions from agriculture, *Climatic Change*, 117, 677–690, doi:10.1007/s10584-012-0593-3, 2013.

20 Shindell, D. T.: Evaluation of the absolute regional temperature potential, *Atmos. Chem. Phys.*, 12, 7955–7960, doi:10.5194/acp-12-7955-2012, 2012.

Shine, K., Fuglestvedt, J., Hailemariam, K., and Stuber, N.: Alternatives to the global warming potential for comparing climate impacts of emissions of greenhouse gases, *Climatic Change*, 68, 281–302, doi:10.1007/s10584-005-1146-9, 2005.

25 Shine, K. P., Berntsen, T. K., Fuglestvedt, J. S., Skeie, R. B., and Stuber, N.: Comparing the climate effect of emissions of short- and long-lived climate agents, *Philos. T. Roy. Soc. A*, 365, 1903–1914, doi:10.1098/rsta.2007.2050, 2007.

Sterner, E., Johansson, D. A., and Azar, C.: Emission metrics and sea level rise, *Climatic Change*, 127, 335–351, doi:10.1007/s10584-014-1258-1, 2014.

30 Strefler, J., Luderer, G., Aboumahboub, T., and Krieglger, E.: Economic impacts of alternative greenhouse gas emission metrics: a model-based assessment, *Climatic Change*, 125, 319–331, doi:10.1007/s10584-014-1188-y, 2014.

Takahashi, K.: The global hydrological cycle and atmospheric shortwave absorption in climate models under CO₂ forcing, *J. Climate*, 22, 5667–5675, doi:10.1175/2009jcli2674.1, 2009.

Thorpe, L. and Andrews, T.: The physical drivers of historical and 21st century global precipitation changes, *Environ. Res. Lett.*, 9, 064024, doi:10.1088/1748-9326/9/6/064024, 2014.

Tol, R. S. J., Berntsen, T. K., O'Neill, B. C., Fuglestvedt, J. S., and Shine, K. P.: A unifying framework for metrics for aggregating the climate effect of different emissions, *Environ. Res. Lett.*, 7, 044006, doi:10.1088/1748-9326/7/4/044006, 2012.

5

ESDD

6, 719–760, 2015

Metrics for linking emissions of gases and aerosols to global precipitation changes

K. P. Shine et al.

Title Page

Abstract

Introduction

Conclusions

References

Tables

Figures



Back

Close

Full Screen / Esc

Printer-friendly Version

Interactive Discussion



Metrics for linking emissions of gases and aerosols to global precipitation changes

K. P. Shine et al.

Table 1. The absolute GWP (in 10^{-14} Wm $^{-2}$ kg $^{-1}$ year), absolute GTP_P (in 10^{-16} Kkg $^{-1}$) and absolute GPP_P (in 10^{-17} mmday $^{-1}$ kg $^{-1}$) for a pulse emission of CO₂ and the GWP, GTP_P and GPP_P, relative to CO₂, for pulse emissions of 4 other species at time horizons of 20 and 100 years.

	GWP(20)	GWP(100)	GTP _P (20)	GTP _P (100)	GPP _P (20)	GPP _P (100)
Absolute CO ₂	2.50	9.19	6.85	5.48	2.27	2.13
CH ₄	84	28	67	4.3	120	8.1
N ₂ O	263	264	276	234	396	325
Sulphate	−141	−38	−41	−5.28	−92	−10.1
Black carbon	2415	657	701	91	1580	173

Title Page

Abstract

Introduction

Conclusions

References

Tables

Figures

◀

▶

◀

▶

Back

Close

Full Screen / Esc

Printer-friendly Version

Interactive Discussion



Metrics for linking emissions of gases and aerosols to global precipitation changes

K. P. Shine et al.

Table 2. The absolute GTP_S (in 10^{-14} $Kkg^{-1}yr$) and absolute GPP_S (in 10^{-15} $mm\ day^{-1}\ kg^{-1}\ yr$) for a sustained emission of CO_2 and the GTP_S and GPP_S , relative to CO_2 , for sustained emissions of 4 other species at time horizons of 20 and 100 years.

	$GTP_S(20)$	$GTP_S(100)$	$GPP_S(20)$	$GPP_S(100)$
Absolute CO_2	1.05	5.90	0.105	1.91
CH_4	93	31.5	357	49.6
N_2O	256	267	846	401
Sulphate	-199	-43.2	-1490	-100
Black carbon	3410	741	-23 500	-979

Title Page

Abstract

Introduction

Conclusions

References

Tables

Figures

◀

▶

◀

▶

Back

Close

Full Screen / Esc

Printer-friendly Version

Interactive Discussion

Metrics for linking emissions of gases and aerosols to global precipitation changes

K. P. Shine et al.

Table 3. The $AGPP_P$ (in $10^{-17} \text{ mm day}^{-1} \text{ kg}^{-1}$) and $AGPP_S$ (in $10^{-15} \text{ mm day}^{-1} \text{ kg}^{-1} \text{ yr}$) for a pulse emission of CO_2 and the GPP_P and GPP_S , relative to CO_2 , for pulse emissions of 4 other species at time horizons of 20 and 100 years, using the values of surface–atmosphere partitioning of radiative forcing from Kvalevåg et al. (2013). The two black carbon values are, respectively, using a model-derived vertical profile for present-day emissions and assuming that the present-day burden is placed entirely at 550 hPa.

	GPP_P (20)	GPP_P (100)	GPP_S (20)	GPP_S (100)
Absolute CO_2	2.99	2.63	0.275	2.53
CH_4	101	6.6	187	44.4
N_2O	370	303	486	367
Sulphate	−70	−8.2	−741	−94.0
Black Carbon	1200	141	−36 600, −87 400	−3740, −9250

Title Page

Abstract

Introduction

Conclusions

References

Tables

Figures

◀

▶

◀

▶

Back

Close

Full Screen / Esc

Printer-friendly Version

Interactive Discussion



Metrics for linking emissions of gases and aerosols to global precipitation changes

K. P. Shine et al.

Table A1. Parameter values used for each species included in calculations. All values are taken from Myhre et al. (2013), unless otherwise stated, and the CH₄ and N₂O values of A_x include the indirect effects described there.

	A_x (W m ⁻² kg ⁻¹)	τ_x (years)	f (Andrews et al., 2010)	f (Kvalevåg et al., 2013)	2008 emissions (kg)
CO ₂	1.76×10^{-15}	See text	0.8	0.6	3.69×10^{13}
CH ₄	2.11×10^{-13}	12.4	0.5	0.3	3.64×10^{11}
N ₂ O	3.57×10^{-13}	121.0	0.5	0.3	1.07×10^{10}
Sulphate	-3.2×10^{-10}	0.011	0.0	-0.4	1.27×10^{11}
Black carbon	3.02×10^{-9}	0.02	2.5	6.2, 13.0	5.31×10^9

Title Page

Abstract

Introduction

Conclusions

References

Tables

Figures

◀

▶

◀

▶

Back

Close

Full Screen / Esc

Printer-friendly Version

Interactive Discussion



Metrics for linking emissions of gases and aerosols to global precipitation changes

K. P. Shine et al.

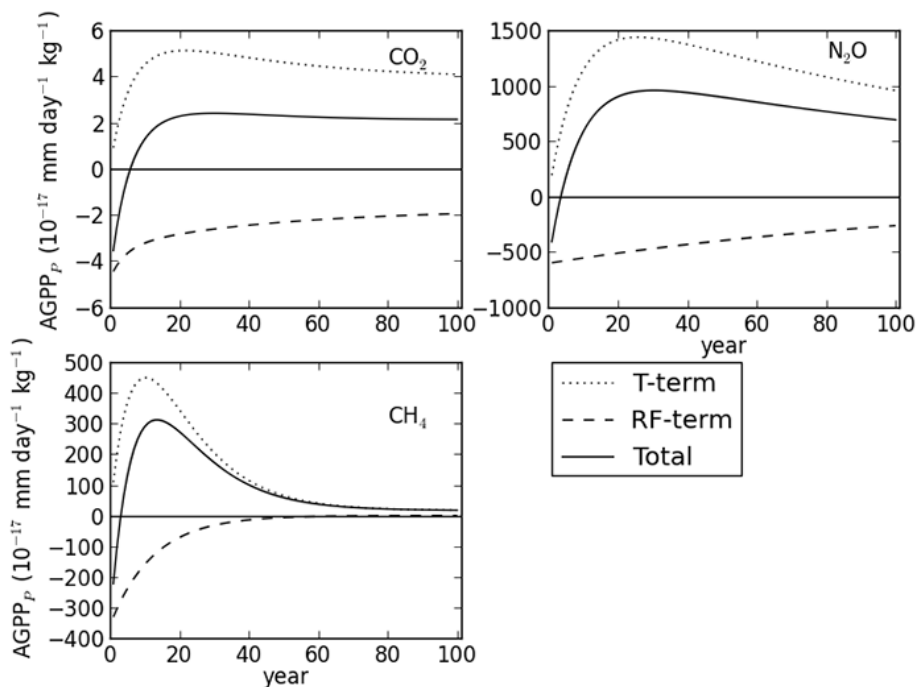


Figure 1. AGPP_p for 1 kg pulse emissions of CO₂, N₂O and CH₄. The *T*-term and RF-term refer to the first and second terms on the right hand side of Eq. (3) respectively, and the Total term is the sum of these.

Metrics for linking emissions of gases and aerosols to global precipitation changes

K. P. Shine et al.

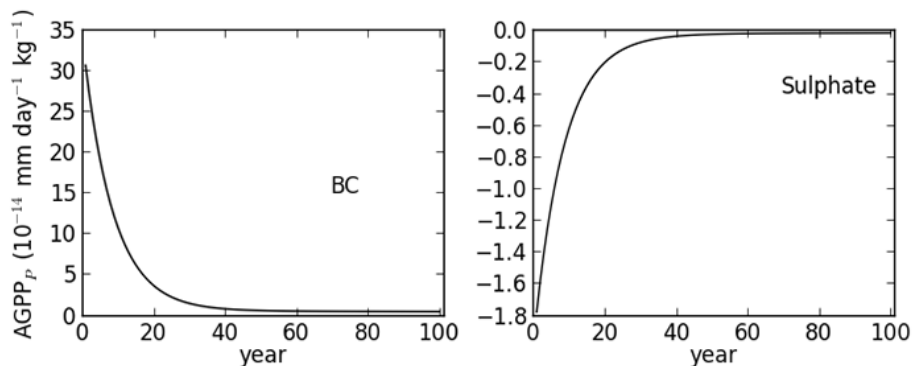


Figure 2. AGPP_p for 1 kg pulse emissions of black carbon (BC) and sulphate. Note that the RF-term in Eq. (3) is negligible for such short-lived gases, except at time horizons less than a few weeks, and only the total is shown.

Title Page

Abstract

Introduction

Conclusions

References

Tables

Figures

◀

▶

◀

▶

Back

Close

Full Screen / Esc

Printer-friendly Version

Interactive Discussion



Metrics for linking emissions of gases and aerosols to global precipitation changes

K. P. Shine et al.

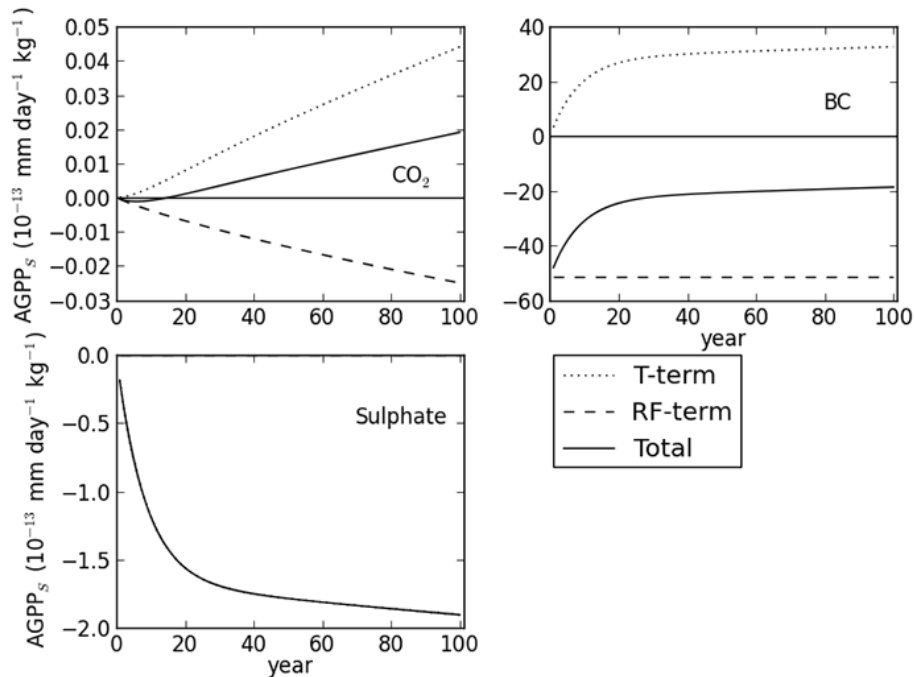


Figure 3. AGPP_s for 1 kg yr⁻¹ sustained emissions of CO₂, BC and sulphate. The *T*-term and RF-term refer to the first and second terms on the right hand side of Eq. (3) respectively, and the Total term is the sum of these. For sulphate, the RF term is assumed to be zero (see text) and so only the Total is shown.

Metrics for linking emissions of gases and aerosols to global precipitation changes

K. P. Shine et al.

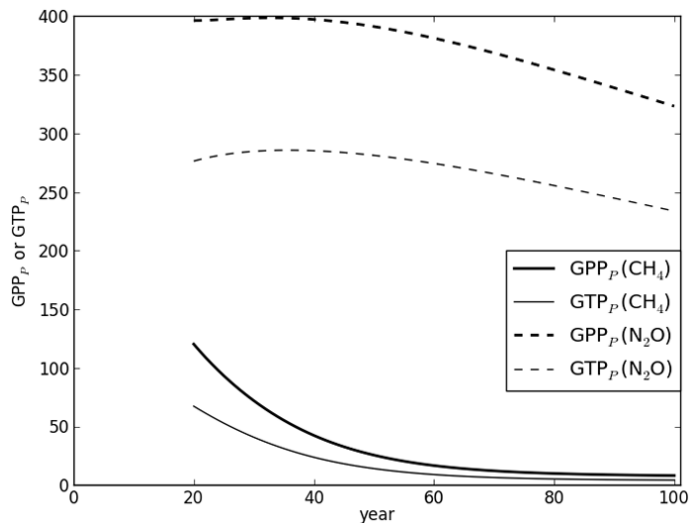


Figure 4. GPP_p (in bold) and GTP_p for 1 kg pulse emissions of N₂O and CH₄ relative to a 1 kg pulse emission of CO₂.

Title Page

Abstract

Introduction

Conclusions

References

Tables

Figures

◀

▶

◀

▶

Back

Close

Full Screen / Esc

Printer-friendly Version

Interactive Discussion



Metrics for linking emissions of gases and aerosols to global precipitation changes

K. P. Shine et al.

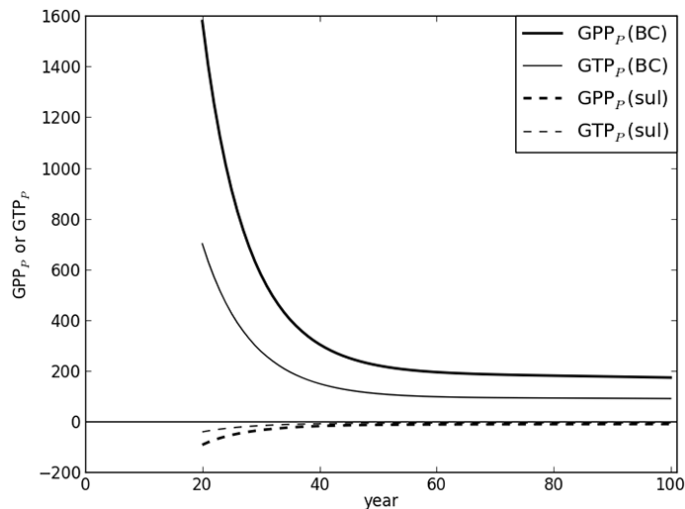


Figure 5. GPP_p (in bold) and GTP_p for 1 kg pulse emissions of BC and sulphate relative to a 1 kg pulse emission of CO_2 .

Metrics for linking emissions of gases and aerosols to global precipitation changes

K. P. Shine et al.

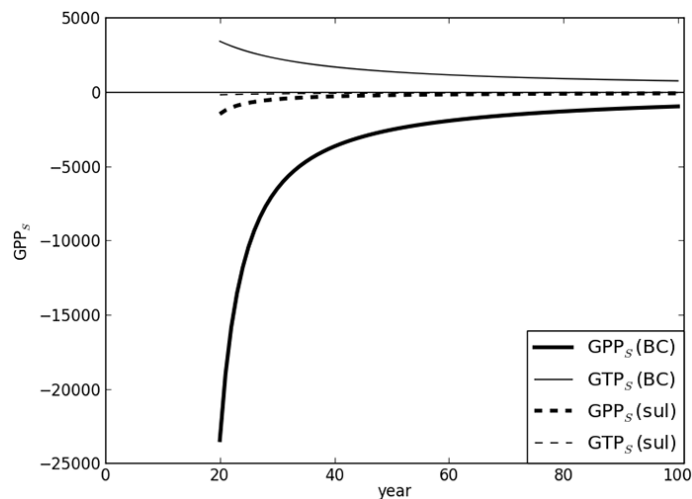


Figure 6. GPP_s (in bold) and GTP_s for 1 kg yr^{-1} sustained emissions of BC and sulphate relative to a 1 kg yr^{-1} sustained emission of CO_2 .

Title Page

Abstract

Introduction

Conclusions

References

Tables

Figures

◀

▶

◀

▶

Back

Close

Full Screen / Esc

Printer-friendly Version

Interactive Discussion



Metrics for linking emissions of gases and aerosols to global precipitation changes

K. P. Shine et al.

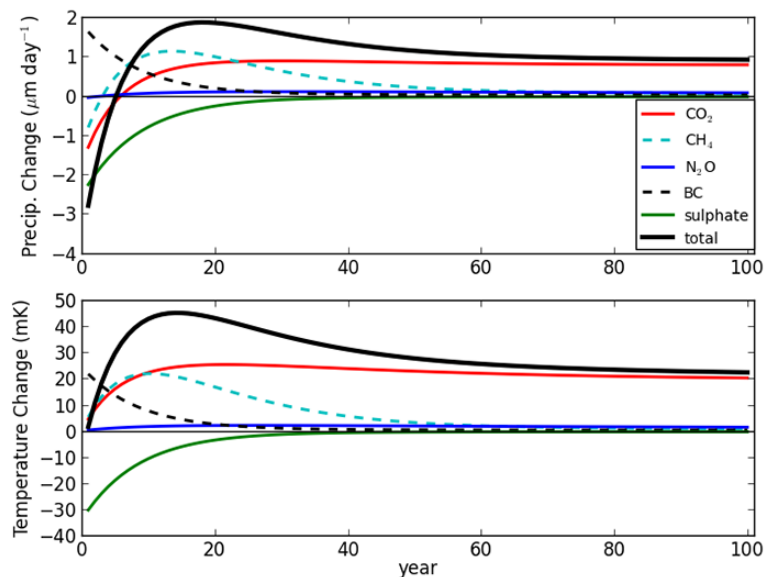


Figure 7. Precipitation change, in $\mu\text{m day}^{-1}$ (top panel), and temperature change, in mK, (bottom panel) in the years after 2008, following a pulse emission in 2008, calculated using the AGPP_P and AGTP_P and using estimated emissions of the species in 2008.

Metrics for linking emissions of gases and aerosols to global precipitation changes

K. P. Shine et al.

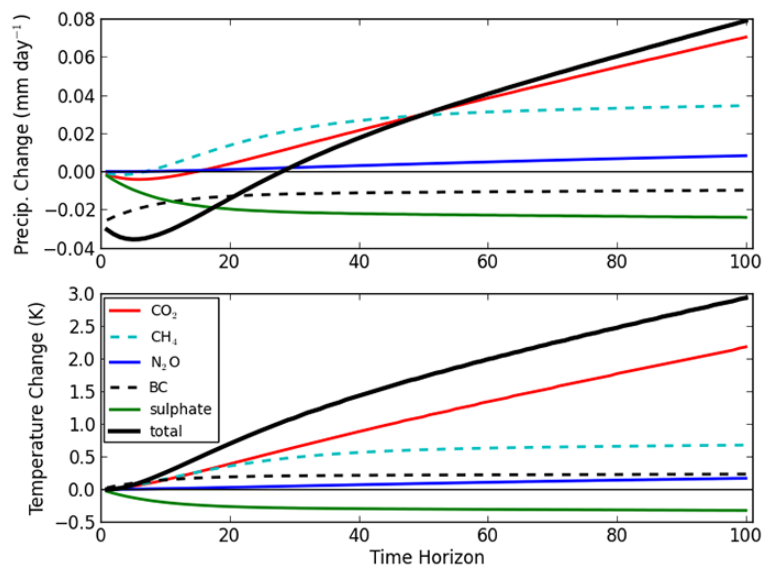


Figure 8. Precipitation change, in mm day^{-1} (top panel), and temperature change, in K, (bottom panel) in the years after 2008, assuming constant emissions at 2008 levels, calculated using the AGPP_S and AGTP_S and using estimated emissions of the species in 2008.

[Title Page](#)[Abstract](#)[Introduction](#)[Conclusions](#)[References](#)[Tables](#)[Figures](#)[⏪](#)[⏩](#)[◀](#)[▶](#)[Back](#)[Close](#)[Full Screen / Esc](#)[Printer-friendly Version](#)[Interactive Discussion](#)

Metrics for linking emissions of gases and aerosols to global precipitation changes

K. P. Shine et al.

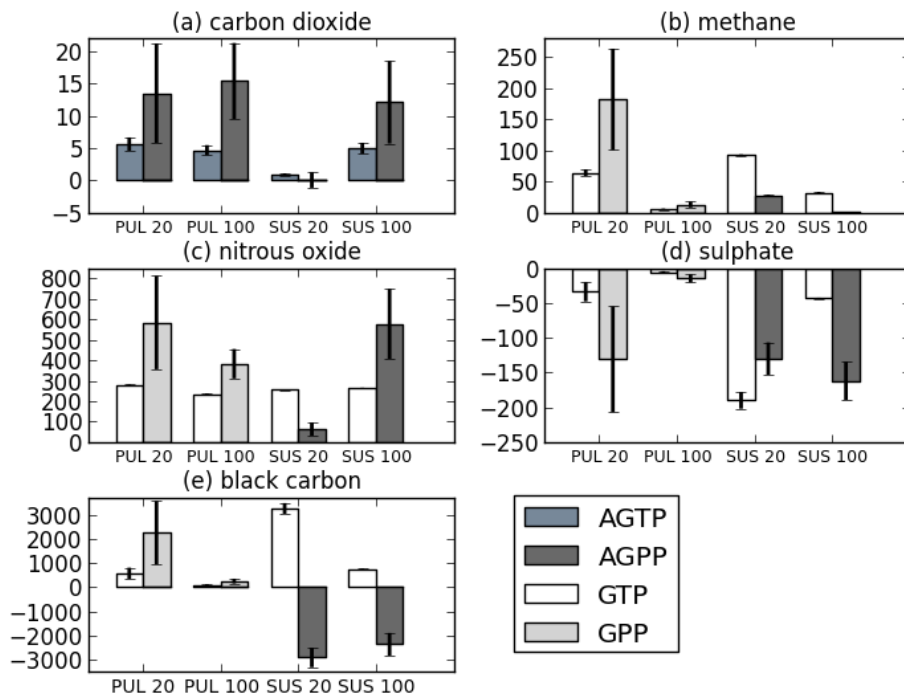


Figure 9. Mean and SDs of the AGTP, AGPP, GTP and GPP for both pulse (PUL) and sustained (SUS) emissions for time horizons of 20 and 100 years, using 18 different representations of the impulse-response function for temperature change. **(a)** AGTP and AGPP for carbon dioxide, for both pulse and sustained emissions, and then GTP_P , GPP_P , GTP_S and $AGPP_S$ for **(b)** methane, **(c)** nitrous oxide, **(d)** sulphate and **(e)** black carbon. For CO_2 the units are $10^{-16} K kg^{-1}$ for $AGTP_P$, $10^{-14} K kg^{-1} yr$ for $AGTP_S$, $10^{-18} mm day^{-1} kg^{-1}$ for $AGPP_P$ and $10^{-16} mm day^{-1} kg^{-1} yr$ for $AGPP_S$. The $AGPP_S$ for all other gases are in $10^{-15} mm day^{-1} kg^{-1} yr$.

Title Page	
Abstract	Introduction
Conclusions	References
Tables	Figures
◀	▶
◀	▶
Back	Close
Full Screen / Esc	
Printer-friendly Version	
Interactive Discussion	